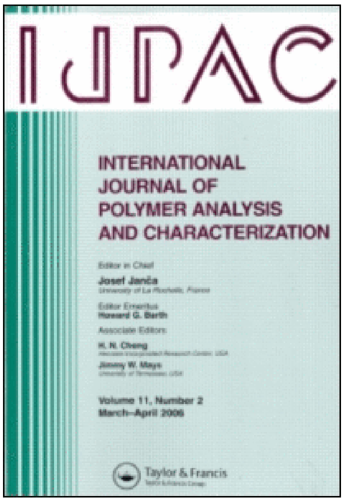

International Journal of Polymer Analysis and Characterization
Publication details, including instructions for authors and subscription information:
http://www.informaworld.com/smpp/title~content=t713646643

Influence of the MWD of Poly(Vinylidene Fluoride) on its Viscoelastic Behavior in the Melt, Part I: Empirical Relationships

Djamel Ayad[a]; Christian Carrot[a]; Jacques Guillet[a]
[a] Laboratoire de Rhéologie des Matières Plastiques, Université Jean Monnet, Saint-Etienne, France

To cite this Article Ayad, Djamel , Carrot, Christian and Guillet, Jacques(2001) 'Influence of the MWD of Poly(Vinylidene Fluoride) on its Viscoelastic Behavior in the Melt, Part I: Empirical Relationships', International Journal of Polymer Analysis and Characterization, 6: 6, 619 — 637

To link to this Article: DOI: 10.1080/10236660108030873

URL: http://dx.doi.org/10.1080/10236660108030873

International Journal of Polymer Anal. Charact., 6: 619–637, 2001

1023-666X/01 $12.00+.00

Influence of the MWD of Poly(Vinylidene Fluoride) on its Viscoelastic Behavior in the Melt, Part I: Empirical Relationships

Djamel Ayad, Christian Carrot, and Jacques Guillet
Laboratoire de Rhéologie des Matières Plastiques,
Université Jean Monnet, Saint-Etienne, France

A deep analysis of the viscoelastic behavior of molten polyvinylidene fluoride (PVDF) was performed in oscillatory shear flow and using isothermal melt spinning. Owing to a thorough analysis of the molecular weight distribution of various samples, empirical relationships relating the observed behavior and parameters of the MWD were obtained. These relations make use of simple and easy-to-handle rheological characteristics such as the crossover frequency and crossover modulus, Newtonian viscosity and relaxation time in shear, and factors such as the melt strength or breaking stretch ratio in extension. For this reason, these relationships may be of interest from an industrial point of view as an aid for tailoring materials or for the design and choice of processing techniques.

Keywords: Viscoelastic behavior; Extension; PVDF; Melt; MWD

1. INTRODUCTION

Polyvinylidenefluoride (PVDF) is a semicrystalline polymer with remarkable properties such as piezo-electrical and pyro-electrical characteristics. In addition, it also has good mechanical properties, chemical resistance, thermal stability until 290°C, combined with good processability. Its dielectric constant reaches high value in the order of 10 at 1 kHz and 20°C.

Received 25 June 1999; In final form 1 May 2000.

Address correspondence to Dr. Christian Carrot, Laboratoire de Rhéologie des Matières Plastiques, Faculté de Sciences et Techniques, Université Jean Monnet, 23, Rue du Docteur Paul Michelon, 42023 Saint-Etienne Cedex 2, France. E-mail: carrot@univ-st-etienne.fr

Because of these exceptional properties, this polymer often finds large industrial applications in the field of chemistry, packaging, cable insulation, or material protecting. However, its main interest lies in the electrical area, especially in the form of thin biaxially oriented or polarized films for capacitors or acoustic devices.

Among the processing methods for the making of these films, extrusion followed by biaxial stretching is the most commonly used. These techniques imply combined and complex flows with large strains and strong nonlinear effects from a thermomechanical point of view.

The understanding of polymer behavior in these complex flows requires a preliminary rheological study in a more simple flow situation. Because for polymer melts the rheological behavior is strongly related to their structures and especially to their molecular weight distribution (MWD), the understanding of the relationships between the parameters that characterize this distribution and the observed behavior in model shear and elongational flows can be of great usefulness for the manufacturer for either the choice or the optimization of both material and process.

Moreover, these relations might confirm the rheology as an additional tool for characterization and analysis of the molecular weight distribution. Indeed, classical methods for this determination require the use of diluted solutions of polymer, which may sometimes be a problem for such chemically resistant materials. On the other hand, the viscoelastic behavior of molten polymers in bulk is very easy to determine and is known to be very susceptible to the molecular weight characteristics of the polymer especially in the entangled zone.

In this study, attention is focused on classical molecular weight analysis of industrial samples of PVDF and on the influence of the molecular weight on the viscoelastic behavior in the melt in two simple flows, namely oscillatory flow in shear and elongational flow using anisothermal spinning.

2. EXPERIMENTAL

2.1. Materials and Molecular Weight Characterization

Six samples of industrial origin are investigated. Five of them (A1, A2, A3, S1, S2) were obtained by suspension polymerization whereas the last one (E) is an emulsion product.

Because the classical analysis of the molecular weight distribution of polymers can only be performed through the study of solutions and because in the case of PVDF this requires the use of polar solvents at relatively high temperature, a deeper investigation of this point has to be performed. Indeed, contradictory results are often reported in the literature[1–4].

In the following experiments, the solutions were obtained at high temperature (80°C) in dimethyl formamide (DMF) for size exclusion chromatography or osmometry and at room temperature (25°C) in dimethyl acetamide (DMAC) for viscosimetry.

The size exclusion chromatography (SEC) analysis was carried out in a Waters device using three columns with a flow rate of 0.5 cm^3/min. The concentration of the solution was approximately 0.01 g/cm^3 and the input for analysis was 200 mm^3. Relative calibration was performed using monodisperse linear polystyrene standards. The window for detection ranges from 4.10^3 to 4.10^7 g/mol.

Lutringer et al.[6–7] have studied industrial and laboratory samples of PVDF dissolved in DMF at 95°C. They measured apparent average molecular weights using polystyrene standards, which were then corrected with a universal calibration curve. They proposed the following relation:

$$\bar{M}_2 = \left(\frac{K_1}{K_2}\right)^{1/1+a_2} \bar{M}_1^{1+a_1/1+a_2} = K\bar{M}_1^a \tag{1}$$

$\bar{M}_1$ and $\bar{M}_2$ are respectively the apparent (PS) and absolute (PVDF) average molecular weights. Relation (1) is obtained from the so-called Mark–Houwink laws, respectively for PS (subscript 1) and PVDF (subscript 2). The K and a values given by Lutringer et al. are then $K = 3.15$ and $a = 0.85$.

Viscosimetry was performed in an Ubbelhode capillary (diameter = 0.6 mm) at 25 ± 0.1°C after diluting the initial concentration of 0.01 g/cm^3. The flow time of the pure solvent was greater than 100 s. According to Lutringer et al.[6,7], the Mark–Houvink relations for PVDF in classical solvents are:

$$[\eta] = 1.95 \times 10^{-2} M_w{}^{0.73} \quad \text{in DMF, } 25^\circ\,\text{C} \tag{2}$$

and

$$[\eta] = 2.15 \times 10^{-2} M_w{}^{0.715} \quad \text{in DMAC, } 25^\circ\,\text{C} \tag{3}$$

with M_w in g/mol and $[\eta]$ in cm^3/g.

These Mark–Houwink laws were confirmed by SEC coupled with light scattering. Moreover, after Lutringer et al.[6,7], the intrinsic viscosity of emulsion products like sample E should be corrected from the microgel volume fraction (f) obtained through the area of the high molecular weight peak depicted on chromatograms from size exclusion chromatography. They proposed the following empirical relation, the efficiency of which was proved when studying several emusion products:

$$[\eta] = [\eta]_a/(1 - f) \tag{4}$$

Osmometry measurements were performed in DMF at 80°C in a Knauer osmometer using cellulose triacetate membranes and dilution from the initial concentration of 0.015 g/cm^3.

2.2. Rheological Characterization of PVDF in the Molten State

Oscillatory shear measurements were performed in a Rheometrics Dynamic Analyser RDA 700 using a parallel plate geometry (diameter = 25 mm, gap = 2 mm) after identifying the linear viscoelastic domain. The explored frequency window ranges from 0.01 to 100 rad/s but temperatures from 200 to 250°C were investigated and enabled the recovery of master curves at 200°C on a larger domain.

Apparent elongational properties were estimated using a melt spinning experiment in nonisothermal condition. A capillary rheometer Instron 3211 was equipped with a capillary die (diameter = 1.25 mm, $L/D = 50$). Extrusion was carried out at 200°C with a flow rate of 7.13 mm^3/s. The extrudate was pulled down with a drawing system located far from the crystallization line at 626 mm from the die exit. The stretching force was measured by a scale with a 0.1 g accuracy and the spin diameter was recorded with an optical device moving along the thread line. Attention has been focused on the melt strength MS (force at break) and breaking stretch ratio BSR (maximum stretching ratio at break). The gravity and the inertial forces were assumed to be negligible so that the rheological force is equal to the stretching force. The apparent elongational viscosity at the freezing point (at a distance L from the die exit) can alternatively be calculated. Indeed, neglecting the variation of the temperature along the spinline, a simple force balance leads to the following relation:

$$\eta_E(\mathrm{ap}) = \frac{F_R L}{Q \ln T_T} \tag{5}$$

where:

F_R is the stretching rheological force
L is the length of the spinline between the exit of the die and the freezing point
Q is the flow rate
T_T is the stretching ratio

3. RESULTS AND DISCUSSION

3.1. Molecular Weight Distribution

Figure 1 shows the chromatograms of four samples (S1, A1, S2, E). For comprehension purposes, these samples were chosen because of the existence of large high molecular weight tails. For example, in the case of the same sample E, Lutringer et al.[6,7] found that the area of the high molecular weight peak depicted on the SEC chromatogram enabled to estimate 6.5% microgel volume fraction. The molecular parameters of Table I are given without any correction and after performing corrections from Equation (1).

These values were also compared with the results of viscosimetry in DMAC at 25°C and osmometry in DMF at 80°C (Table II), and this shows the reliability of the corrections performed on the SEC values.

3.2. Shear Experiments

Figures 2 and 3 show a plot of the oscillatory results, either in terms of dynamic shear moduli or real part of the complex viscosity for samples S1

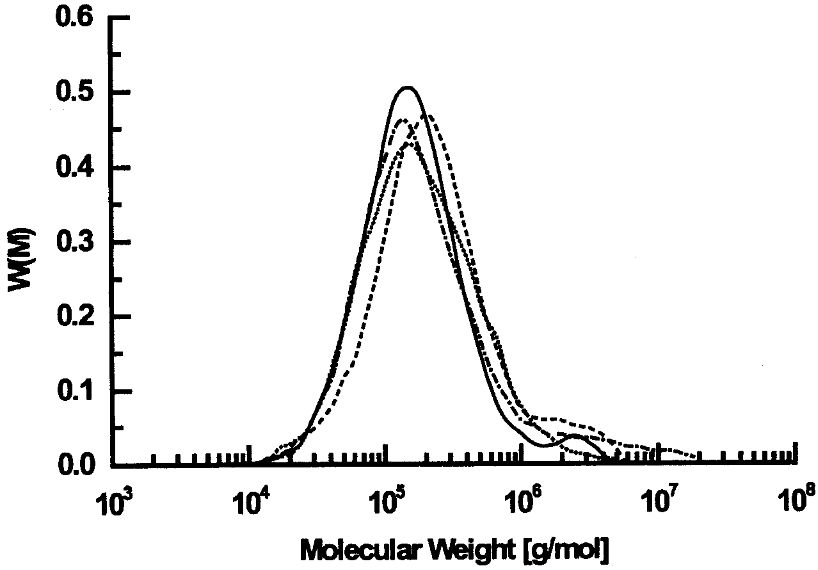

FIGURE 1 Chromatograms of PVDF samples in DMF at 80°C (—: S1, - - -: A1, · · ·: S2, —·—: E).

TABLE I Molecular Characteristics of the Samples (from SEC in DMF at 80°C)

	Non-Corrected			Absolute Values (after correction)		
Sample	M_w [g/mol]	M_n [g/mol]	M_w/M_n	M_w [g/mol]	M_n [g/mol]	M_w/M_n
S1	252000	108000	2.3	123000	60000	2.1
A1	273000	110000	2.5	131000	61000	2.2
A2	328000	132000	2.5	153000	71000	2.2
A3	330000	118000	2.8	154000	64000	2.4
S2	380000	131000	2.9	174000	71000	2.5
E	483000	112000	4.3	213000	62000	3.5

and E, which represent two extreme cases of molecular weight distribution. The experimental results were compared with the Cole–Cole[8] and Carreau–Yasuda[9–10] equations for the complex viscosity because these expressions are commonly used for modeling purposes. The relevant parameters were obtained by minimization of the chi-square function between the loss and storage modulus values and the equation derived from the complex viscosity. Indeed, for the Cole–Cole equation:

$$\eta^* = \frac{\eta_0}{1 + (j\omega\bar{\lambda})^{1-h}} \tag{6}$$

where η_0 is the zero-shear viscosity, $\bar{\lambda}$ is a characteristic relaxation time, and h is a distribution parameter (between 0 and 1).

The results are given in Table III and show the susceptibility of the zero-shear viscosity and relaxation time to the molecular weight distribution while the distribution parameter remains rather insensitive to it,

TABLE II Molecular Characteristics of the Samples (From Viscosimetry in DMAC at 25°C and Osmometry in DMF at 80°C)

	Viscosimetry		Osmometry	
Sample	$[\eta]$ [cm^3/g]	M_v [g/mol]	Viriel Coeff. [mol cm^3 g^{-2}]	M_n [g/mol]
S1	94.0	124000	0.000011	61000
A1	105.0	145000	0.0000096	68000
A2	114.0	162000	0.0000096	76000
A3	110.5	155000	0.000011	66000
S2	114.5	163000	0.0000096	71000
E	124.0	183000	0.0000086	62000

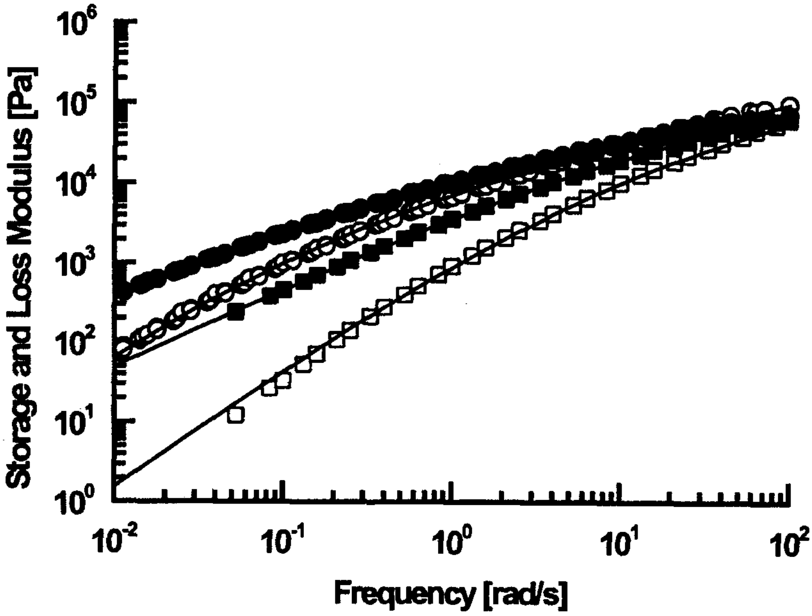

FIGURE 2 Storage (filled symbols) and loss modulus (open symbols) of samples S1 (■, □) and sample E (●, ○) at 200°C from experiments and calculation (—) from Eq. (6).

probably because of the narrow range of the polydispersity index explored. The full lines on Figure 2 are the predicted values of equation 6 with the parameters of Table III. Though the model gives a good estimate of the zero shear viscosity, it is not useful for obtaining any other viscoelastic parameter, since the predicted limiting slope of the loss and storage moduli in a double logarithmic plot are respectively 1-*h* and 2-*h*, in contradiction with the predictions of the linear viscoelasticity for which these slopes should be 1 and 2. Moreover, a constant value of the plateau modulus in the plateau zone is not predicted by this type of equation.

The Carreau–Yasuda equation gives the following mathematical form for the real part of the complex viscosity:

$$\eta' = \frac{\eta_0}{\left[1+(\omega\lambda_0)^{2a}\right]^{(1-n)/(2a)}} \qquad (7)$$

where η_0 is the zero-shear viscosity, λ_0 is a characteristic relaxation time, n is the flow index at high shear rates, and a characterizes the smoothness of the transition between the Newtonian and non-Newtonian behavior.

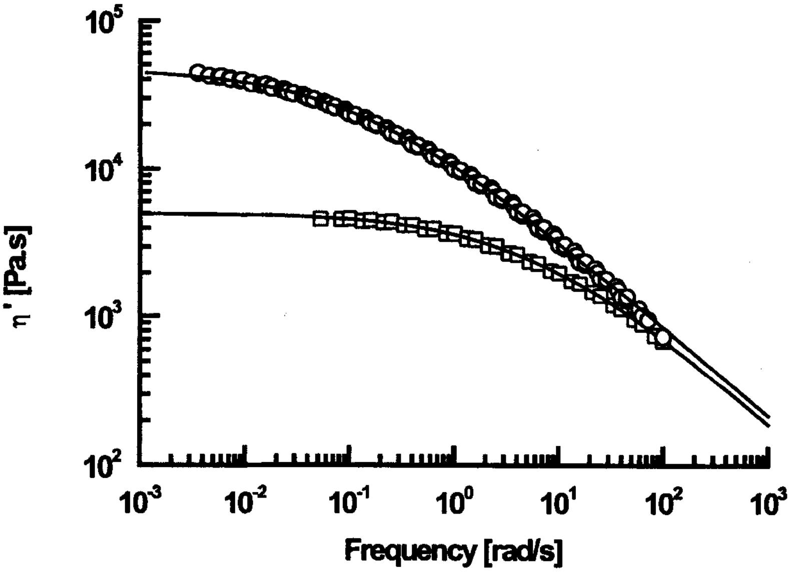

FIGURE 3 Real part of the complex viscosity of samples S1 (□) and sample E (○) at 200°C from experiments and calculation (—) from Eq. (7).

The calculated parameters are reported in Table III; the Newtonian viscosity and characteristic relaxation time are similar to those of the Cole–Cole model and parameters *a* and *n* remain constant for the range of polydispersity under investigation. Figure 3 shows an example of the results that were obtained from this model for the real part of the complex viscosity of samples S1 and E.

TABLE III Model Parameters at 200°C

	Equation (6)			Equation (7)			
Sample	η_0 [Pa s]	$\bar{\lambda}$ [s]	*h*	η_0 [Pa s]	λ_0 [s]	*a*	*n*
S1	5060	0.21	0.50	5000	0.19	0.30	0.38
A1	7930	0.21	0.51	7730	0.18	0.30	0.39
A2	16100	0.58	0.51	15600	0.44	0.29	0.37
A3	17500	1.24	0.51	17100	1.09	0.30	0.41
S2	29000	2.20	0.51	28800	1.88	0.30	0.38
E	46500	8.53	0.52	47100	8.18	0.29	0.40

Although both models do not have any theoretical basis and can only describe the viscosity behavior in a limited frequency range, our results show that they may be very useful for the study of polydisperse materials since they offer very simple equations containing reliable parameters which are related to the molecular weight characteristics of the sample.

3.3. Nonisothermal Melt Spinning Experiments

Figure 4 shows the results of the extensional force as a function of the stretching ratio. The extensional force increases slightly and it reaches a plateau at high stretching ratio. This has already been reported by many authors for polyethylenes[11,12]. Moreover the rheological force and the MS increases with the weight, average molecular weight, whereas an opposite trend is noticed for the BSR. Indeed, sample E has very poor properties as far as extensibility is concerned. The results for the BSR and MS are reported in Table IV.

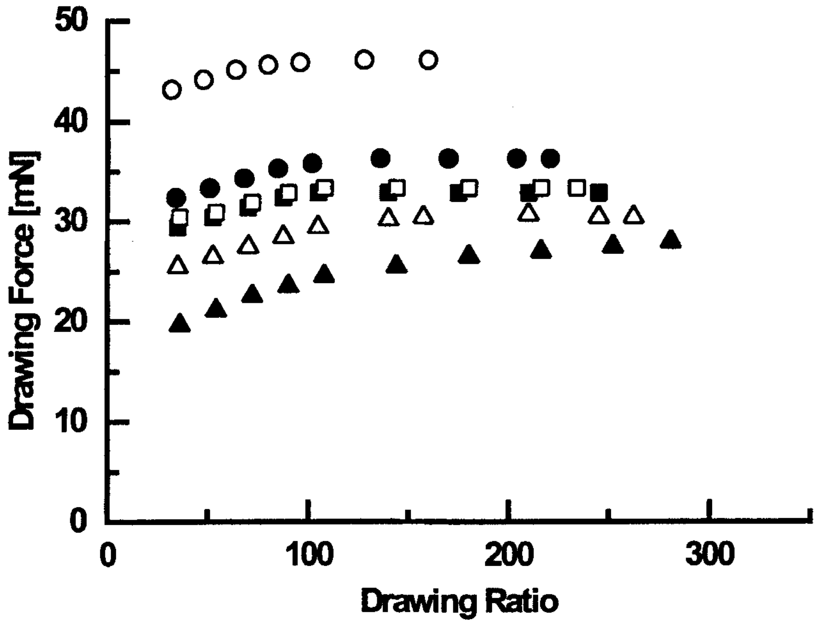

FIGURE 4 Results of melt spinning at 200°C (▲: S1, △: A1, ■: A2, □: A3, ●: 2, ○: E).

3.4. Structure Property Relationships in Shear

From the previous results, some useful relation connecting the microstructure of the polymers with their rheological behavior in the melt can be inferred. Especially, the parameters from the Cole–Cole and Carreau–Yasuda equations can be related to the MWD characteristics. The Newtonian viscosity as obtained from the Cole–Cole plot was shown to be classically dependent on the weight average molecular weight following the scaling law at 200°C:

$$\eta_0 = 1.6 \times 10^{-17} M_w^{4.04} \tag{8}$$

with η_0 in Pa s and M_w in g/mol.

The value of the exponent is higher than the expected value of 3.4[13]; however, it is known that this value is only reliable in the case of monodisperse polymers, whereas the polydispersity generally increases it. Moreover, the shape of the distribution can also have a drastic influence. Following Dobkowski[14,15] and assuming the factorization of the effect of the molecular weight and of the polydispersity together with a fixed value of the exponent of the scaling law of 3.4 enables the writing of

$$\eta_0 = 3.7 \times 10^{-14} M_w^{3.4} \left(\frac{M_w}{M_n}\right)^{0.0034} \tag{9}$$

with η_0 in Pa s and M_w in g/mol, M_w/M_n being the polydispersity index. This shows that the dependence among the polydispersity remains small in the experimental range.

A similar assumption leads to the following equation for the relaxation time

$$\bar{\lambda} = 3.0 \times 10^{-19} M_w^{3.4} \left(\frac{M_w}{M_n}\right)^{2.493} \tag{10}$$

with $\bar{\lambda}$ in s and M_w in g/mol.

TABLE IV Melt Spinning Parameters at 200°C

Sample	MS (mN)	BSR
S1	28.0	280
A1	30.4	260
A2	32.8	245
A3	33.4	235
S2	36.3	220
E	46.1	160

The values of the Newtonian viscosity and characteristic relaxation time calculated by Equations (9) and (10) are compared with the experimental values on Figures 5a and 5b.

The global influence of the MWD on the flow curve is made easier by plots of the normalized viscosity η^*/η_0. Indeed, according to Equations (9) and (10), the plot of the normalized viscosity as a function of the product $\omega \cdot \eta_0$ (Figure 6a) enables it to cancel the effect of the average molecular weight, whereas it clearly shows the effect of the polydispersity. On the other hand, a plot of the same quantity as a function of $\omega \cdot \bar{\lambda}$ (Figure 6b) yields a single mastercurve that confirms the dependence of the relaxation time towards the polydispersity. From these results, one could write an equation

$$\eta^* = \frac{\eta_0}{\left[1 + (\omega\bar{\lambda})^{0.58}\right]^{-0.89}} \tag{11}$$

with the parameters of Equation (7) being $a = 0.3$ and $n = 0.5$.

At high shear rates, the viscosity scales as $\omega^{-0.51}$ as mentioned by other authors [16].

Additionally, the storage and loss moduli variation can also be used for obtaining information on the MWD. Indeed it has been stated that the coordinates (ω_c, G_c) of the crossover point of the moduli yields respectively some evaluation of the molecular weight and polydispersity index[17]. Also, the separation between the moduli ω_{sep}, defined as the ratio of the frequency of the storage and loss modulus curves at an arbitrary given value of the moduli in the terminal zone, is generally assumed to be a good indication of the polydispersity index[18]. The values of the crossover frequency and modulus are given in Table V together with the separation between the moduli. For the latter, the arbitrary value of the modulus was chosen to be 1,000 Pa, which ensures that all the values are taken within the terminal zone.

In the present case, the crossover frequency was found to be well correlated with the weight average molecular weight according to

$$M_w = 4.4 \times 10^5 \omega_c^{-0.28} \tag{12}$$

with M_w in g/mol and ω_c in rad/s.

The polydispersity index was found to be related to the crossover modulus according to a relation similar to that of Zeichner and Patel[19]

$$M_w/M_n = K + 10^5/(KG_c) \tag{13}$$

with G_c in Pascals and $K = 1.1$.

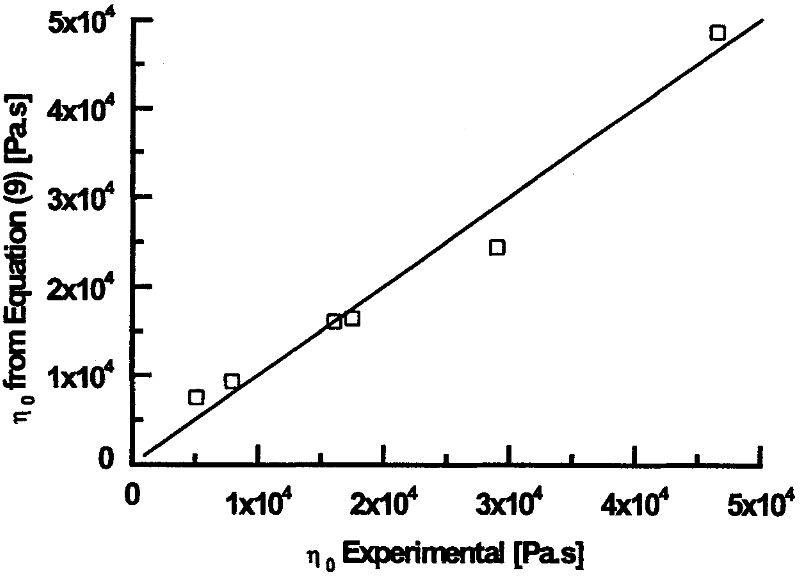

FIGURE 5a Comparison between experimental viscosities and values from Eq. (9).

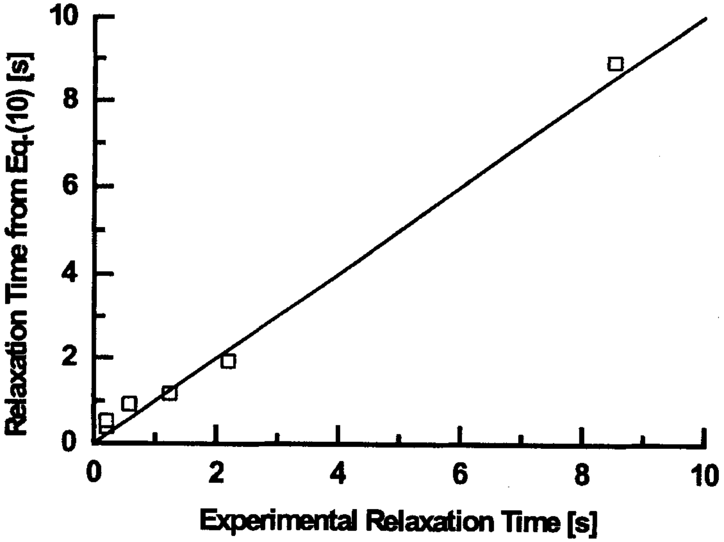

FIGURE 5b Comparison between experimental relaxation times and values from Eq. (10).

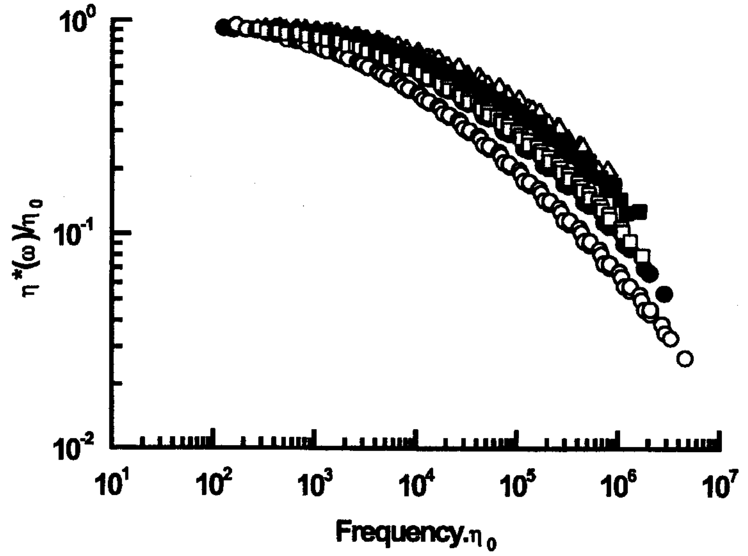

FIGURE 6a Effect of the polydispersity displayed by reduced flow curves (▲: S1, Δ: A1, ■: A2, □: A3, ●: S2, ○: E).

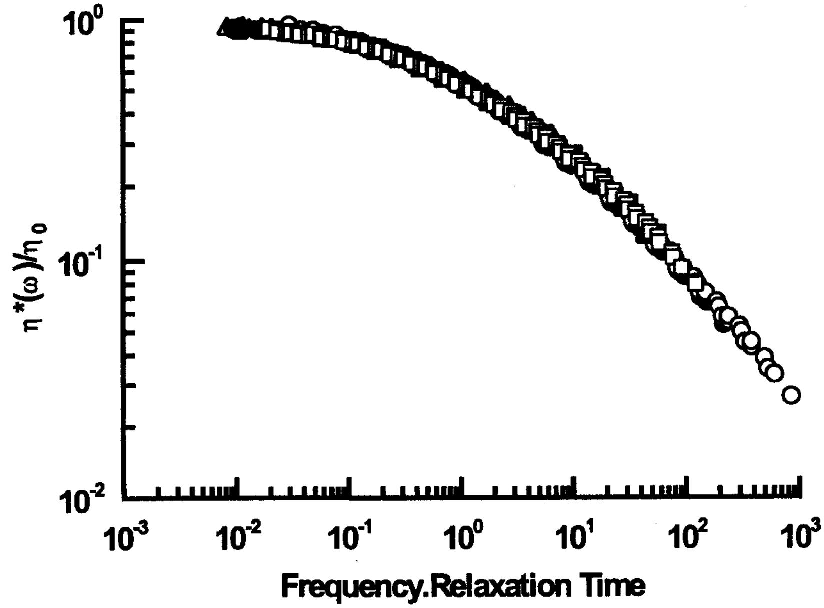

FIGURE 6b Reduced master flow curves (▲: S1, Δ: A1, ■: A2, □: A3, ●: S2, ○: E).

TABLE V: Crossover and Separation Modulus at 200°C

Sample	ω_c [rad/s]	G_c [MPa]	ω_{sep}
S1	>100	Undefined	4.95
A1	79.0	0.089	4.81
A2	44.1	0.087	4.77
A3	42.8	0.068	4.15
S2	27.0	0.066	4.06
E	13.9	0.039	3.00

It should be noted that sample S1 does not show any crossing point in the range of the frequency that was used in this study. In this case the separation between moduli should be preferably used. Indeed, in the present case

$$M_w/M_n = 10.47/\omega_{\text{sep}} \tag{14}$$

These relations are plotted on Figures 7a, 7b, and 7c.

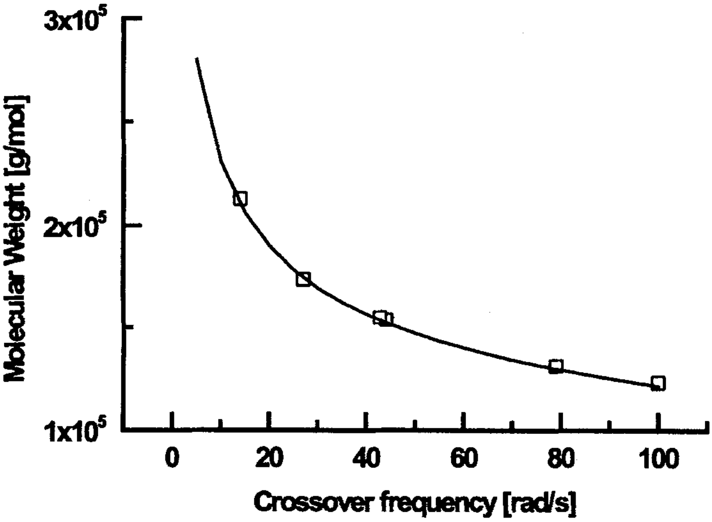

FIGURE 7a Relation between the crossover frequency and the weight average molecular weight, full line according to Eq. (12).

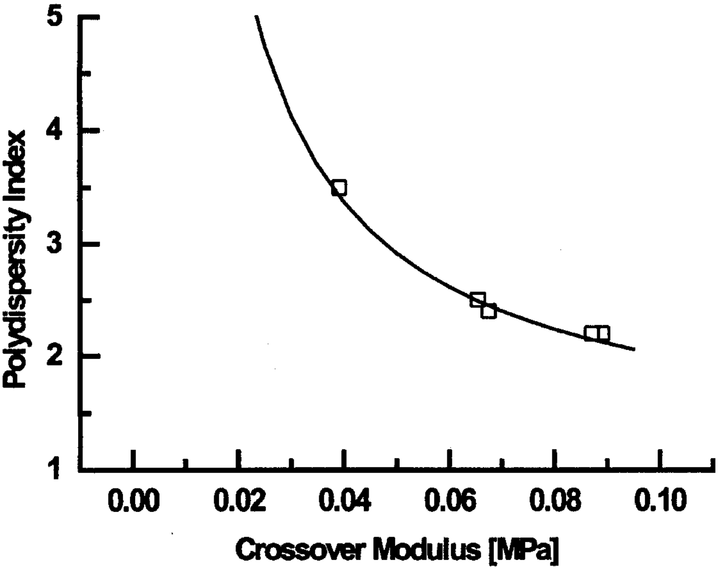

FIGURE 7b Relation between the crossover modulus and the polydispersity index, full line according to Eq. (13).

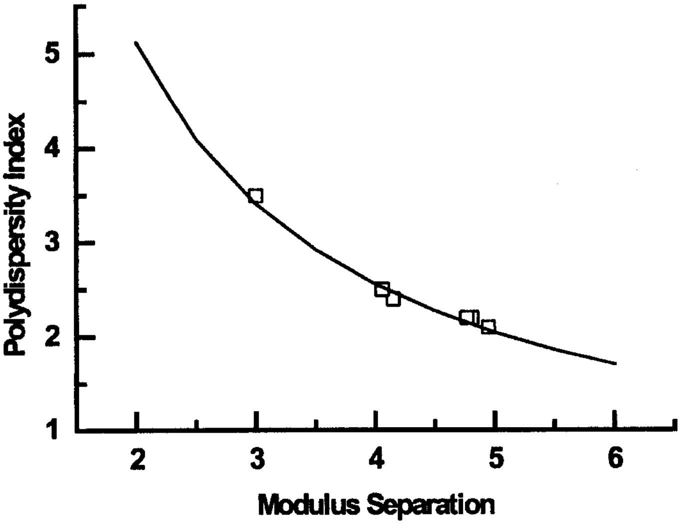

FIGURE 7c Relation between the separation between the moduli and the polydispersity index, full line according to Eq. (14).

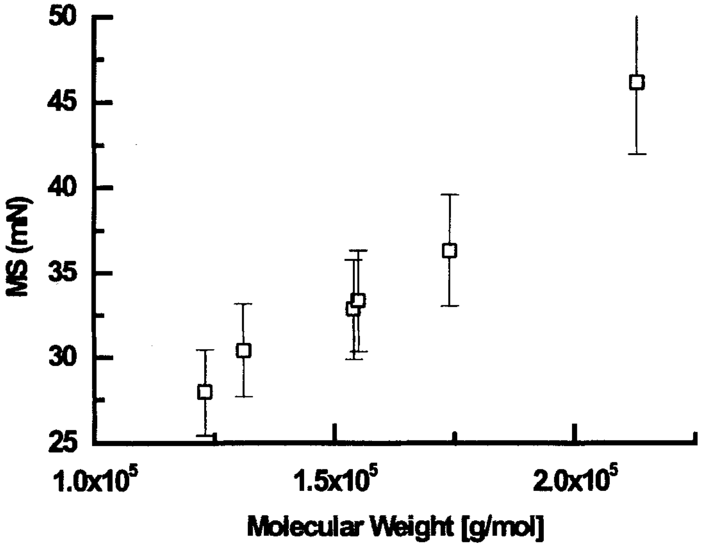

FIGURE 8a Correlation between the melt strength and the weight average molecular weight.

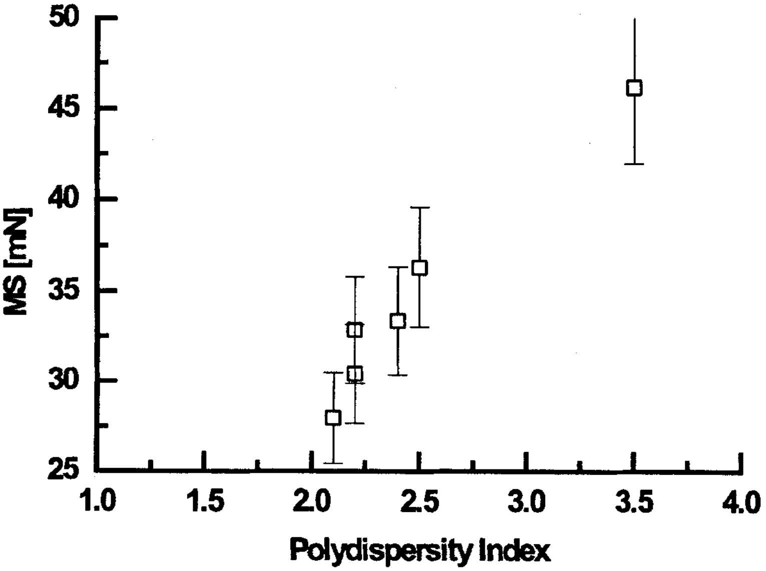

FIGURE 8b Correlation between the melt strength and the polydispersity index.

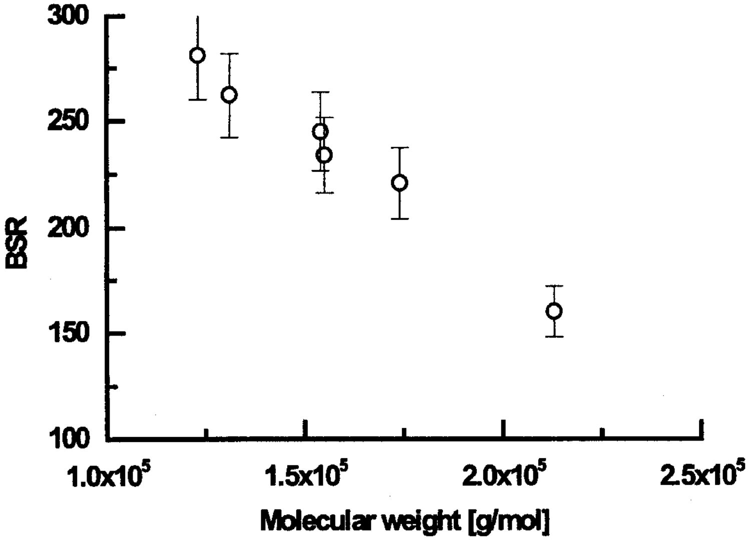

FIGURE 9a Correlation between the BSR and the weight average molecular weight.

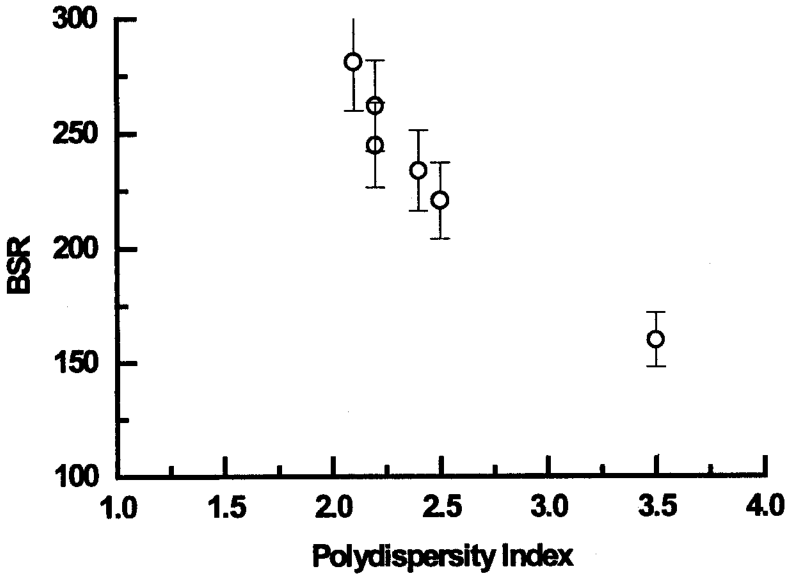

FIGURE 9b Correlation between the BSR and the polydispersity index.

3.5. Structure Property Relationships in Melt Spinning

The influence of the molecular weight and polydispersity is recovered when dealing with the properties of the molten polymers in extension. Indeed, as shown in Figures 8a, 8b, 9a, and 9b, the melt strength and breaking stretch ratio are correlated with these parameters. However the respective contribution of the molecular weight and polydispersity can hardly be distinguished. As a general rule, it may be asserted that the increase of one parameter or the other reduces the extensibility and strengthens the melt as already noted by various authors [20].

4. CONCLUSION

Owing to a complete analysis of the molecular weight distribution of various PVDF samples by means of size exclusion chromatography, osmometry, and viscosimetry in connection with oscillatory experiments in shear and melt spinning in extension, reliable relationships between some parameters of the MWD (polydispersity index and weight average molecular weight) and various rheological characteristics of the molten PVDF were obtained from an empirical point of view.

- The Newtonian viscosity and crossover frequency were found to be related to the weight average molecular weight as expected.
- The crossover modulus or the separation of the modulus in the terminal zone are related to the polydispersity index.
- The terminal relaxation time was found to be related to both parameters; however its dependence towards the average molecular weight is similar to that of the Newtonian viscosity.
- In consequence, the plot of the reduced viscosity (η/η_0) as a function of the reduced frequency ($\omega \cdot \eta_0$) cancels the effect of the molecular weight and emphasizes that of the polydispersity.
- On the other hand, the plot of the reduced viscosity (η/η_0) as a function of the reduced frequency ($\omega \cdot \bar{\lambda}$) yields a single mastercurve independently of the molecular weight and polydispersity at least for similar shapes of the MWD.
- The relative influence of the MWD parameters on the extensional behavior is strong but can hardly be separated.

This set of relation may be of great help as a first step for the tailoring of the molecular weight of PVDF in view of specific processing techniques, and it might also be used for the prediction of the rheological behavior and especially of flow curves from the knowledge of MWD parameters.

REFERENCES

[1] G. J. Welch, (1974). *Polymer*, **15**, 429 (1974).
[2] S. Ali and A. K. Raina, *Makrom. Chem.*, **179**, 2925 (1978).
[3] L. E. Stillwagon, Org. *Coatings, Appl. Sci. Proc.*, **48**, 780 (1983).
[4] R. C. Ferguson and D. W. Ovenoll, *Polym. Preprints*, **340**, (1984).
[5] G. C. Galin, G. Lutringer, and M. Galin, *J. Appl. Polym. Sci.*, **37**, 487 (1989).
[6] G. Lutringer and G. Weill, *Polymer*, **32**, 877 (1991).
[7] G. Lutringer, B. Meurer, and G. Weill, *Polymer*, **32**, 884 (1991).
[8] K. S. Cole and R. H. Cole, *J. Chem. Phys.*, **9**, 314 (1941).
[9] P. J. Carreau, *Trans. Soc. Rheol.*, **16**, 99 (1972).
[10] K. Yasuda, R. C. Armstrong, and R. E. Cohen, *Rheol. Acta*, **20**, 163 (1981).
[11] F. P. Lamantia and D. Acierno, *Polym. Eng. Sci.*, **25**, 279 (1985).
[12] D. Acierno, A. Brancaccio, D. Curto, F.P. Lamantia, and A. Valenza, *J. Rheol.*, **29**, 323 (1985).
[13] M. Doi, *J. Polym. Sci.: Poly. Lett. Ed.*, **19**, 265 (1981).
[14] Z. Dobkowski, *Eur. Polym. J.*, **17**, 1131 (1981).
[15] Z. Dobkowski, *Eur. Polym. J.*, **18**, 1051 (1982).
[16] M. Doi, J. *Non-Newt. Fluid Mech.*, **23**, 151 (1987).
[17] M. Fleissner, *Makrom. Chem., Macrom. Symp.*, **61**, 324 (1992).
[18] M. J. Yoo, Polymer Processing Society, IX Annual Meeting, Manchester, United Kingdom, 5–8 April 1993.
[19] G. R. Zeichner and P. D. Patel, *J. Rheol.*, **26**, 93 (1982).
[20] E. Deprez and W. J. Bontink, *Polym. Rheol. Plast. Proc.*, **274**, 1979.